Electronic Supplementary Material (ESI) for Green Chemistry.
This journal is © The Royal Society of Chemistry 2021

Electronic supplementary information

Amoeba-Inspired Reengineering of Polymer Networks

Yuanbo Zhong, Panpan Li, Xu Wang,* and Jingcheng Hao

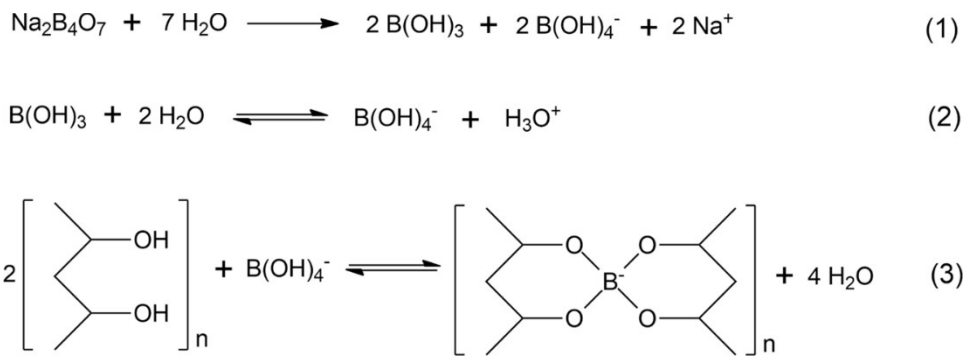

Fig. S1 Possible mechanisms of the reactions between borax and PVA.

Hydrogel optimization

To optimize the yeast-containing, borax-crosslinked PVA hydrogels, the yeast concentration was first kept constant (13 mg/mL), and the borax and PVA concentrations were varied. As shown in Fig. S2a, the very low borax and PVA concentrations led to the formation of sols, and higher concentrations resulted in the formation of hydrogels. When the yeast and PVA concentrations were kept constant (13 and 50 mg/mL, respectively), the rheological moduli of the hydrogels increased with increasing borax concentrations (Fig. S2b). However, as borax was a basic compound, the systems with high concentrations of borax became insensitive to the acid gas-induced transient liquification. Therefore, a moderate concentration of borax (13 mg/mL) was used to yield polymer hydrogels with both good mechanical properties and high sensitivity to the acid gas-induced transient liquification. When the yeast and borax concentrations were fixed (13 and 13 mg/mL, respectively), the rheological moduli of the hydrogels increased with increasing PVA concentrations (Fig. S2c). We adjusted the system pH to 4, which led to a solation of the hydrogels. The viscosities of the sols were measured, and the results were shown in Fig. S2d. We found that the system with a high PVA concentration had a high viscosity, which may hinder the uniform doping of small molecules and nanomaterials during the fuel-driven reengineering process. Fig. S2e showed that the fuel-driven transient liquification became inefficient when the PVA concentration in the hydrogels was high (100 mg/mL). This may be attributed to the limited diffusional process of chemical fuels in the hydrogels with high rheological moduli and viscosity. Therefore, a moderate concentration of PVA (50 mg/mL) was selected as the optimal condition.

Next, the borax and PVA concentrations were fixed to be 13 and 50 mg/mL, respectively, and the yeast concentration was varied. The results in Fig. S3a showed that the rheological moduli of the hydrogels slightly increased with increasing yeast concentrations. The lifetime of the transient sols slightly increased with decreasing yeast concentrations in the concentration range of 13-52 mg/mL (Fig. S3b, c). When the yeast concentration was very low (3 mg/mL), the lifetime of the transient sols became extremely long (Fig. S3c). This was attributed to the slow CO_2 generation within the low yeast concentration in the system. As the lifetimes of the transient sols were close to each other for the yeast concentrations of 13, 26 and 52 mg/mL (Fig. S3c), we chose the lower one (13 mg/mL) as the optimal yeast concentration for further studies.

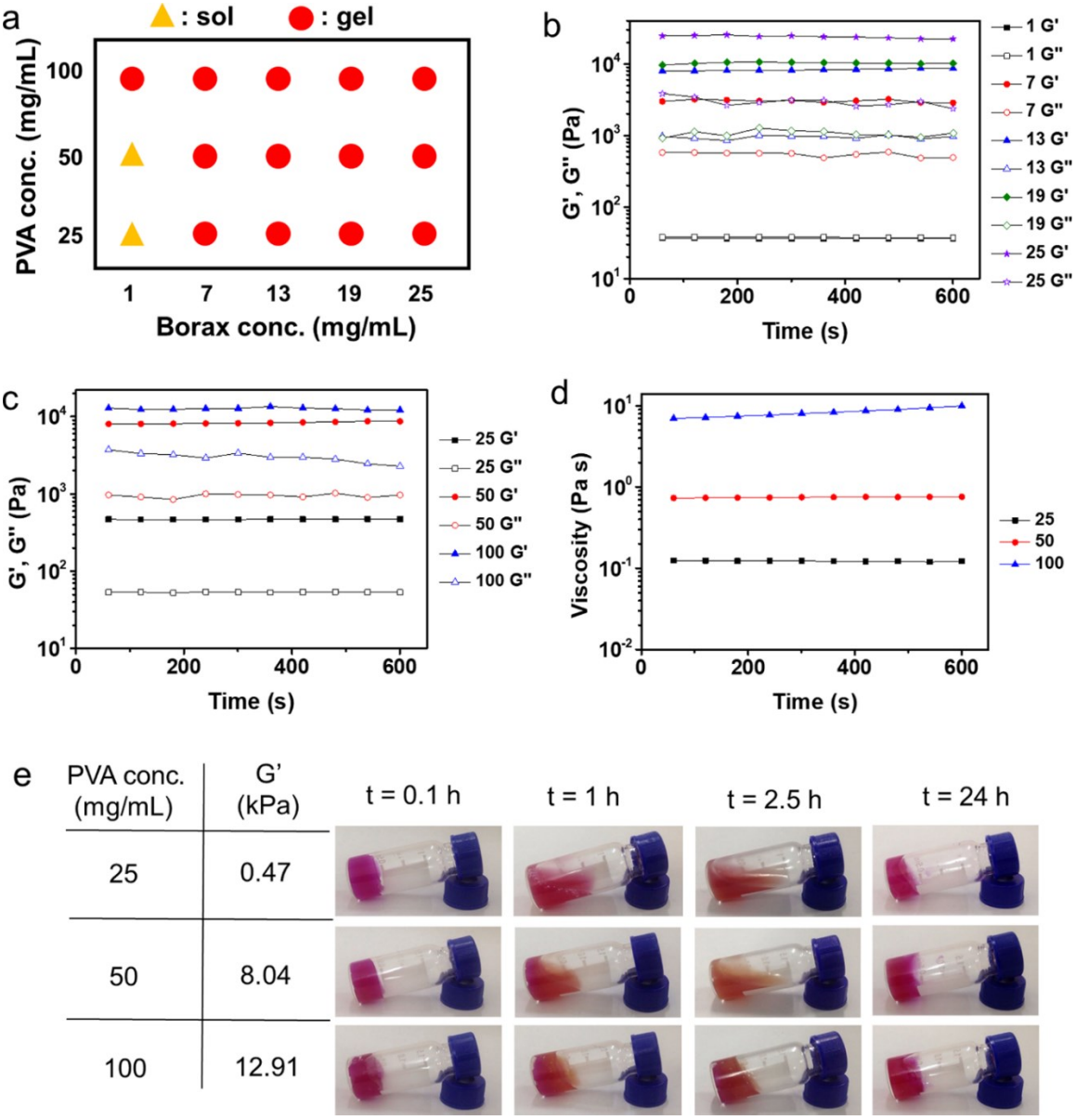

Fig. S2 (a) Phase diagram of the yeast-borax-PVA aqueous systems with a constant yeast concentration (13 mg/mL). (b) Rheological characterization of the yeast-borax-PVA systems with constant yeast and PVA concentrations (13 and 50 mg/mL, respectively) and different borax concentrations (1, 7, 13, 19, and 25 mg/mL). (c) Rheological characterization of the yeast-containing, borax-crosslinked PVA hydrogels with constant yeast and borax concentrations (13 and 13 mg/mL, respectively) and different PVA concentrations (25, 50, and 100 mg/mL). (d) Viscosity of the yeast-borax-PVA systems under pH 4 with constant yeast and borax concentrations (13 and 13 mg/mL, respectively) and different PVA concentrations (25, 50, and 100 mg/mL). (e) The transient liquification behaviors of the yeast-containing, borax-crosslinked PVA hydrogels with different PVA concentrations.

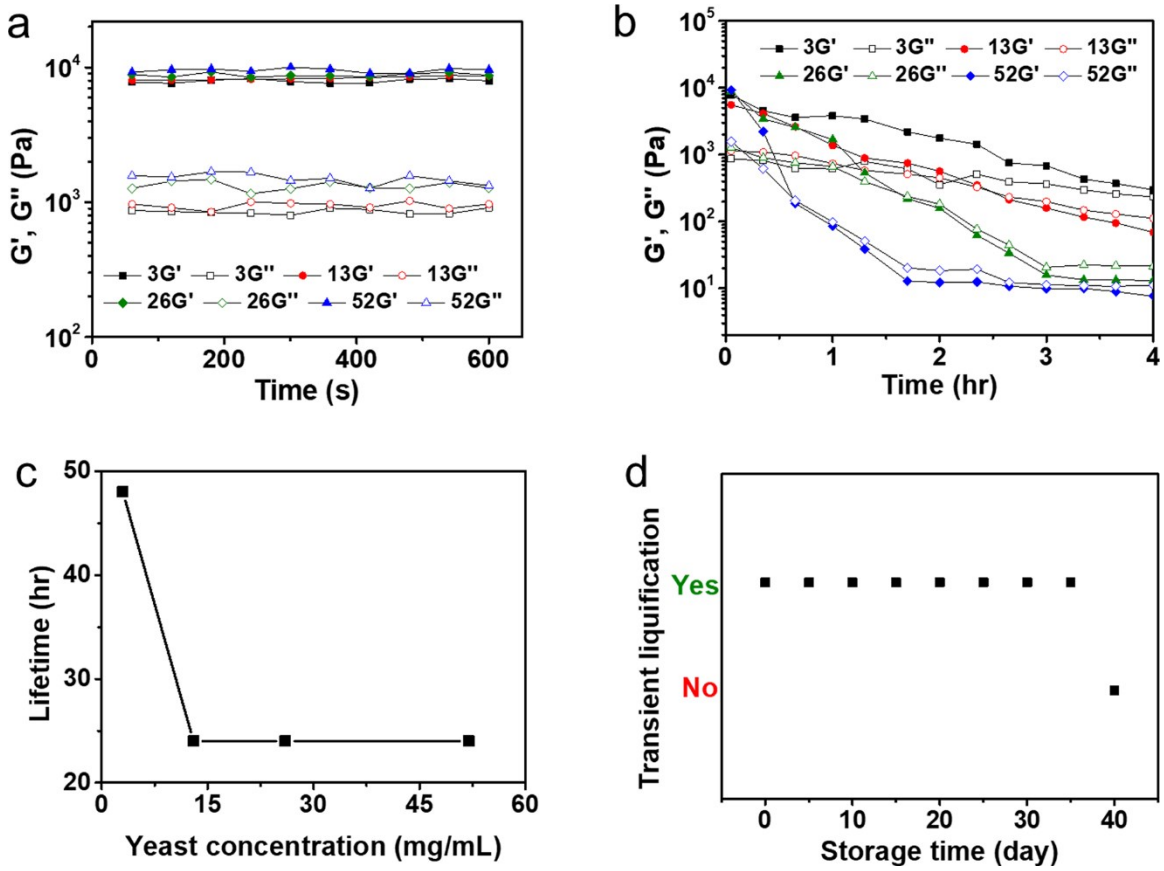

Fig. S3 (a) Rheological characterization of the yeast-containing, borax-crosslinked PVA hydrogels with constant borax and PVA concentrations (13 and 50 mg/mL, respectively) and different yeast concentrations (3, 13, 26, and 52 mg/mL). (b) Variation of rheological moduli with time for the yeast-borax-PVA aqueous systems (initial pH 9) with different yeast concentrations (3, 13, 26, and 52 mg/mL). (c) Lifetime of the transient sols for yeast-borax-PVA aqueous systems (initial pH 9) with different yeast concentrations. (d) The sugar-fueled transient liquification of the yeast-containing, borax-crosslinked PVA hydrogels can occur within 35 days.

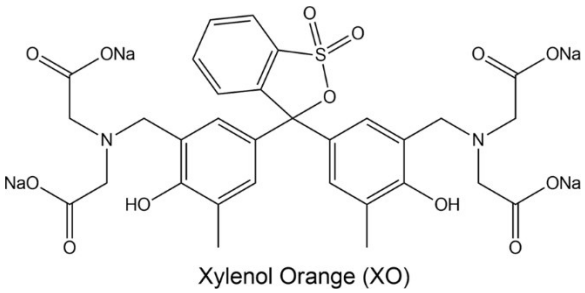

Fig. S4 The chemical structure of XO.

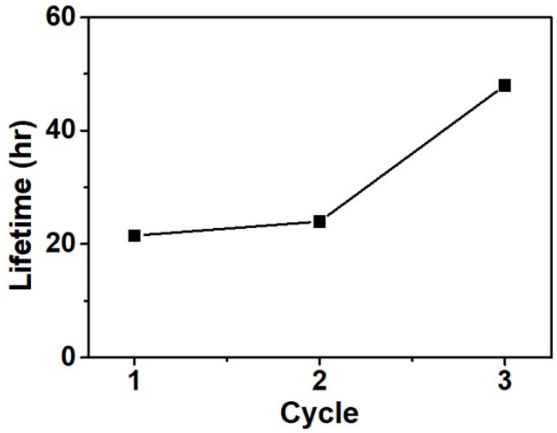

Fig. S5 Lifetimes of the transient sols formed by repeated fuel addition (sucrose concentration 0.1 M).

Fig. S6 Photographs showing the yeast-containing, borax-crosslinked PVA hydrogels can be simply reshaped by fuel-driven transient liquefaction.

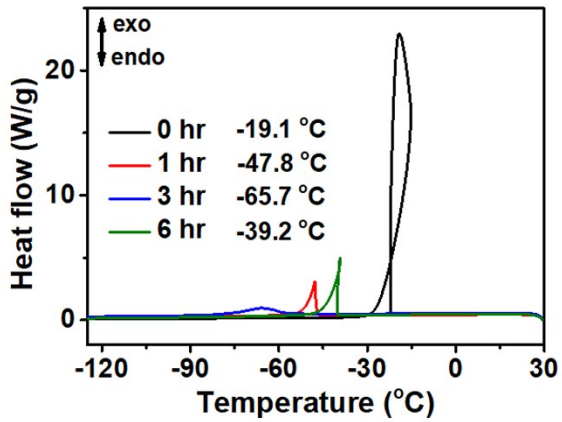

Fig. S7 DSC curves of the yeast-containing, borax-crosslinked PVA hydrogels after liquid exchange with glycol for different time.

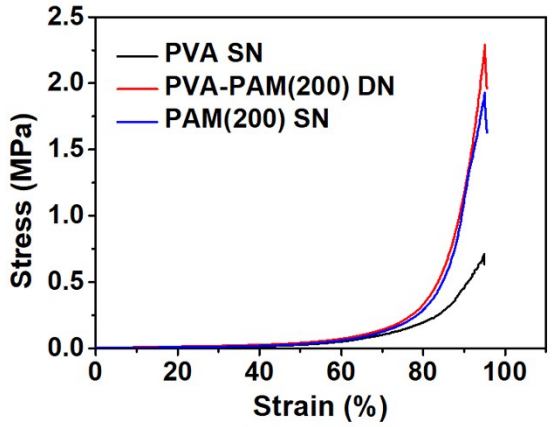

Fig. S8 Representative compressive stress versus compressive strain curves of PVA and PAM (200 mg/mL of AM) single network (SN) hydrogels, and PVA-PAM (200 mg/mL of AM) double network (DN) hydrogels.

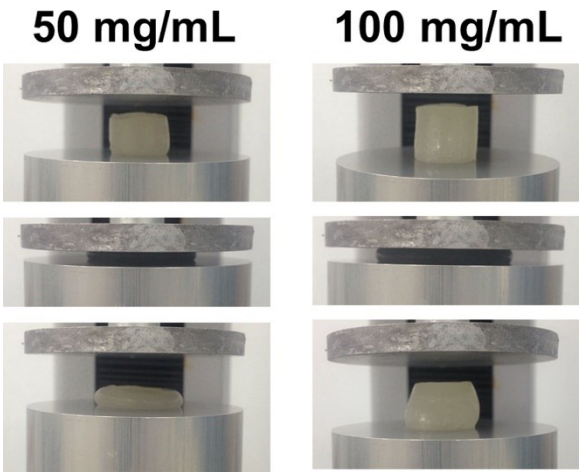

Fig. S9 Photographs showing the deformation of PVA-PAM double network hydrogels with (left) 50 and (right) 100 mg/mL of AM after compression.

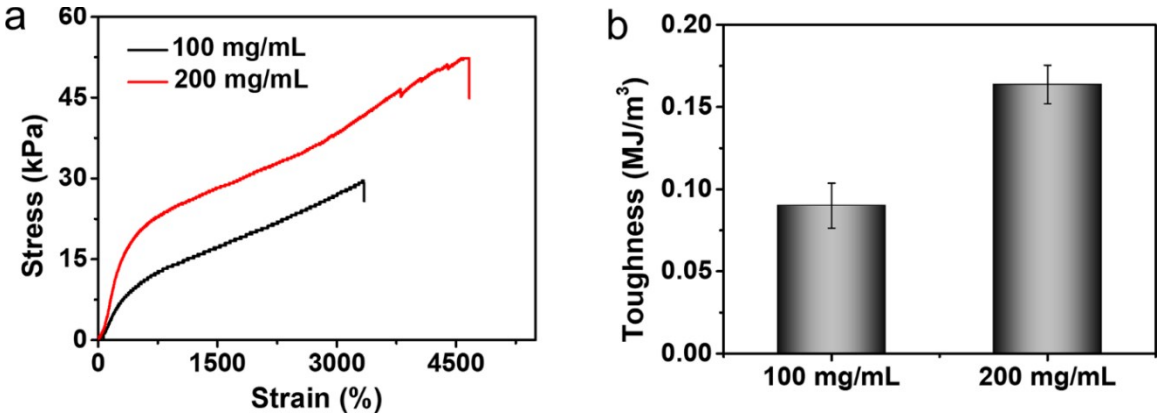

Fig. S10 (a) Representative stress versus strain curves of PVA-PAM double network hydrogels with 100 and 200 mg/mL of AM. (b) Toughness of PVA-PAM double network hydrogels with 100 and 200 mg/mL of AM.

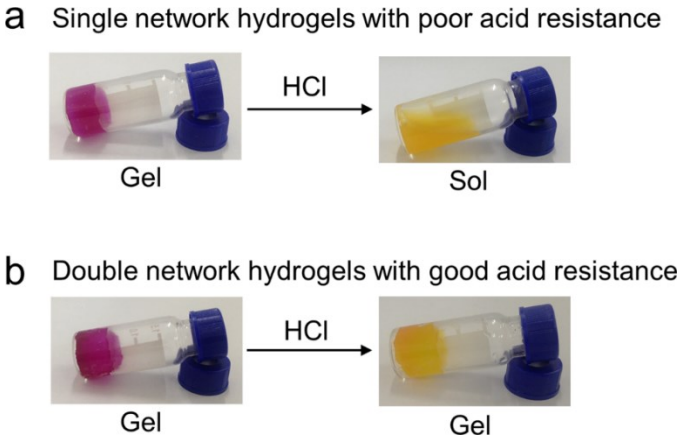

Fig. S11 Photographs showing the poor and good acid resistance for (a) PVA single network and (b) PVA-PAM (200 mg/mL of AM) double network hydrogels, respectively.

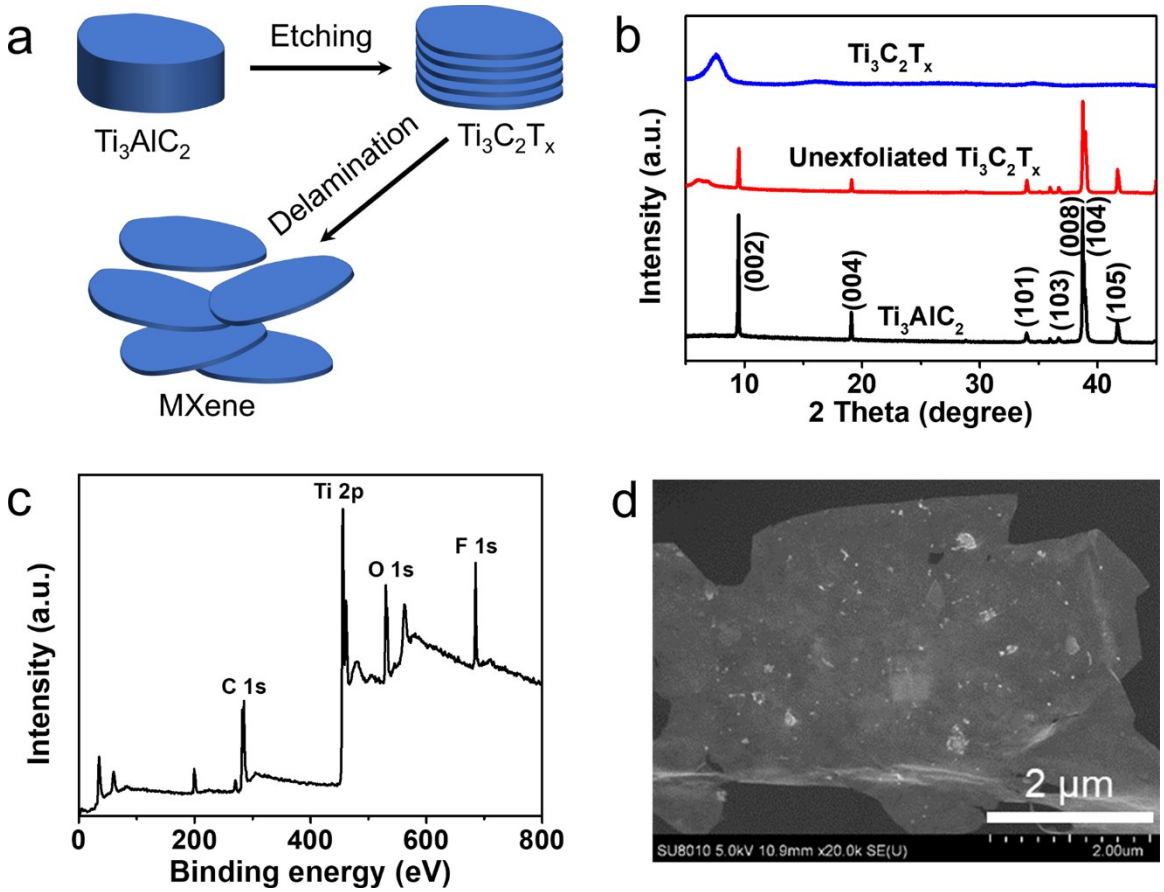

Fig. S12 (a) Schematic description of the synthesis of MXene. (b) XRD patterns of Ti_3AlC_2, unexfoliated $Ti_3C_2T_x$, and exfoliated $Ti_3C_2T_x$ sheets. (c) XPS spectrum of $Ti_3C_2T_x$. (d) SEM image of delaminated MXene nanosheet.

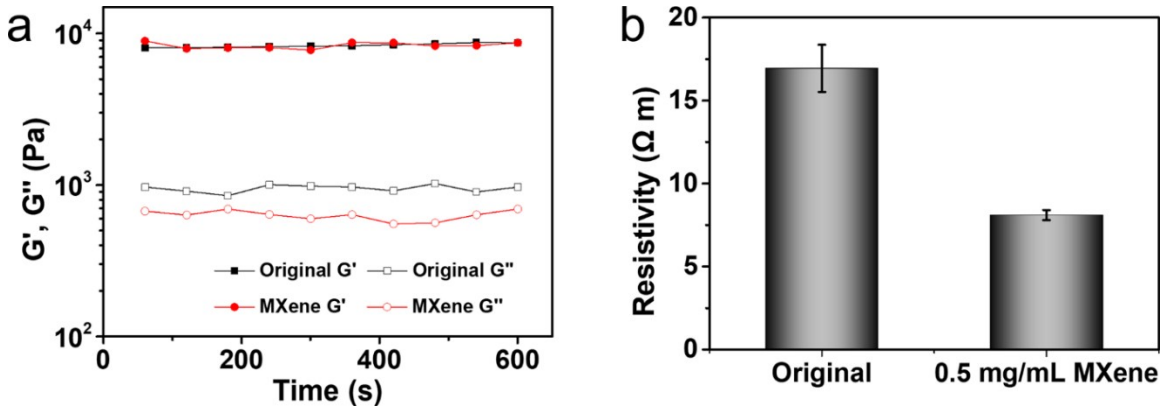

Fig. S13 (a) Rheological characterization of the yeast-containing, borax-crosslinked PVA hydrogels before and after loading of MXene (final concentration 0.5 mg/mL). (b) Resistivity of the yeast-containing, borax-crosslinked PVA hydrogels before and after loading of MXene (final concentration 0.5 mg/mL) under room temperature.

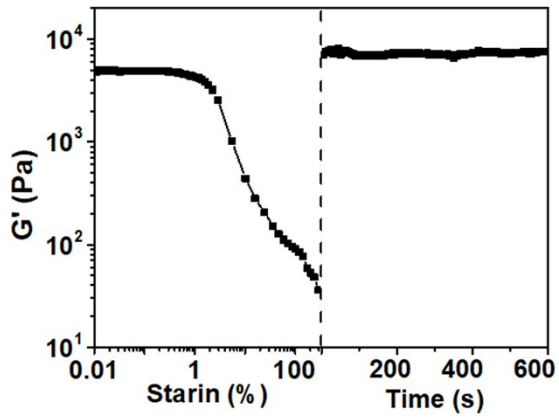

Fig. S14 Dynamic rheology data showing the self-healing ability of the MXene-incorporated, yeast-containing, borax-crosslinked PVA hydrogels.

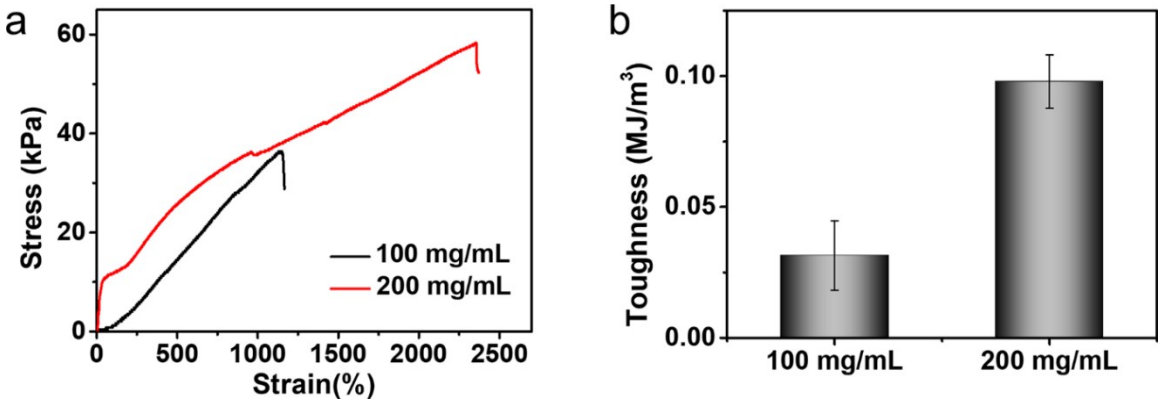

Fig. S15 (a) Representative stress versus strain curves of MXene-incorporated, PVA-PAM double network organohydrogels with 100 and 200 mg/mL of AM. (b) Toughness of MXene-incorporated, PVA-PAM double network organohydrogels with 100 and 200 mg/mL of AM.

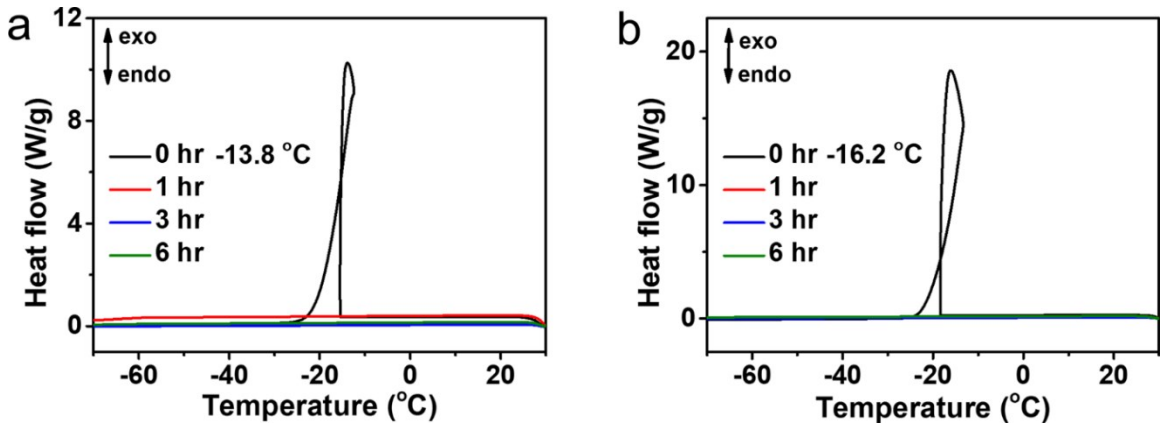

Fig. S16 DSC curves of the PVA-PAM double network hydrogels with (a) 100 and (b) 200 mg/mL of AM after liquid exchange with glycol for different time.

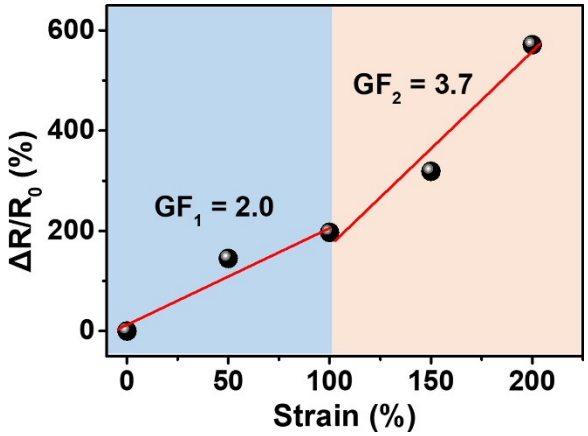

Fig. S17 Response of a MXene-containing, PVA-PAM double network organohydrogel sensor (AM concentration 200 mg/mL) under different strains.

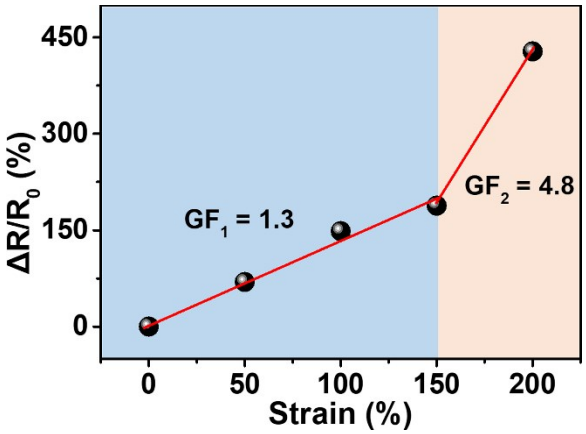

Fig. S18 Response of a PVA-PAM double network organohydrogel sensor without MXene (AM concentration 100 mg/mL) under different strains.

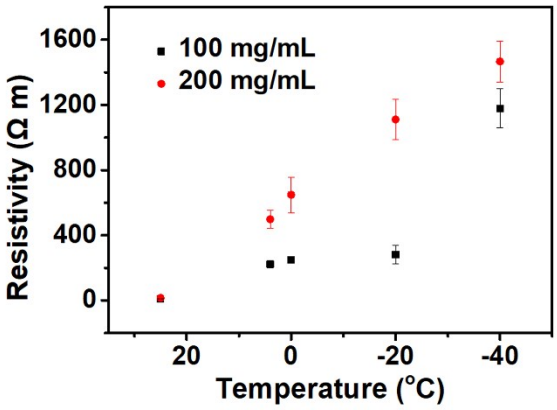

Fig. S19 Resistivity of the MXene-containing PVA-PAM double network organohydrogel sensors with different AM concentrations between the temperature ranges of 25 to -40 °C.

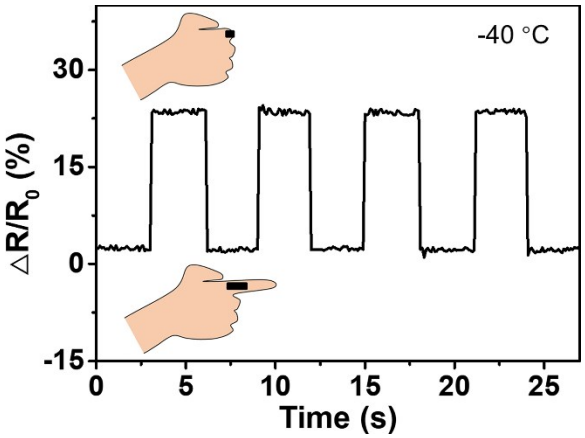

Fig. S20 Response of a MXene-containing, PVA-PAM double network organohydrogel sensor (AM concentration 200 mg/mL) in monitoring finger bending and straightening at -40 °C.

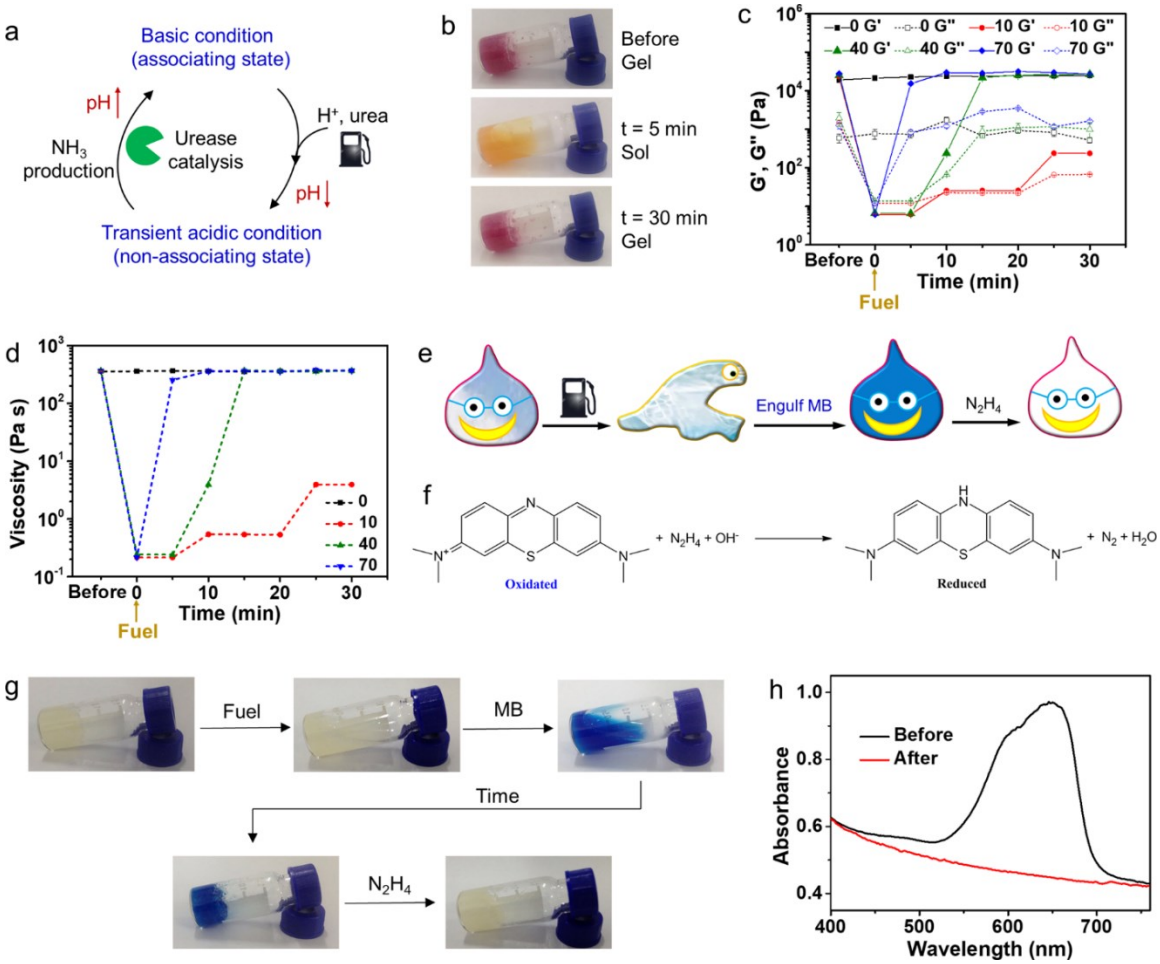

Fig. S21 (a) Schematic illustration of fuel-driven transient liquefaction of supramolecular polymer hydrogels. (b) XO-containing urease-NPCS aqueous systems before and after fuel (3.3% acetic

acid with 40 mg/mL of urea) addition for different time. (c, d) Variation of (c) rheological moduli and (d) viscosity with time for urease-NPCS aqueous systems (initial pH 9) after the addition of fuels with different urea concentrations in mg/mL. (e) Schematic illustration of the incorporation of redox-responsive methylene blue (MB) in polymer hydrogels via fuel-driven transient liquefaction. (f) Reaction between MB and N_2H_4. (g) Photographs showing the processes of MB incorporation and MB reduction by N_2H_4. (h) UV-vis spectra of MB-incorporated NPCS hydrogels before and after N_2H_4 treatments.

Supporting movies

Movie 1 Magnetic response of the Fe_3O_4 nanoparticle-incorporated materials fabricated by fuel-driven reengineering of polymer hydrogels.

Movie 2 Fast and reversible magnetic actuation of the Fe_3O_4 nanoparticle-incorporated materials fabricated by fuel-driven reengineering of polymer hydrogels.